Biologically Compatible Neural Interface To Safely Couple Nanocoated Electrodes to the Surface of the Brain

Elisa Castagnola,[†,*] Alberto Ansaldo,[†] Emma Maggiolini,[†] Gian Nicola Angotzi,[†] Miran Skrap,[‡] Davide Ricci,[†,*] and Luciano Fadiga[†,§]

[†]Robotics, Brain and Cognitive Sciences Department, Istituto Italiano di Tecnologia, Genoa, Italy, [‡]Struttura Operativa Complessa di Neurochirurgia, Azienda Ospedaliero—Universitaria Santa Maria della Misericordia, Udine, Italy, and [§]Section of Human Physiology, University of Ferrara, Ferrara, Italy

ABSTRACT The ongoing interest in densely packed miniaturized electrode arrays for high-resolution epicortical recordings has induced many researchers to explore the use of nanomaterial coatings to reduce electrode impedance while increasing signal-to-noise ratio and charge injection capability. Although these materials are very effective, their use in clinical practice is strongly inhibited by concerns about the potential risks derived from the use of nanomaterials in direct contact with the human brain. In this work we propose a novel approach to safely couple nanocoated electrodes to the brain surface by encapsulating them with a biocompatible hydrogel. We prove that fibrin hydrogel coating over nanocoated high-density arrays of epicortical microelectrodes is electrically transparent and allows avoiding direct exposure of the brain tissue to the nanocoatings while maintaining all the advantages derived from the nanostructured electrode surface. This method may make available acute and sub-acute neural recordings with nanocoated high-resolution arrays for clinical applications.

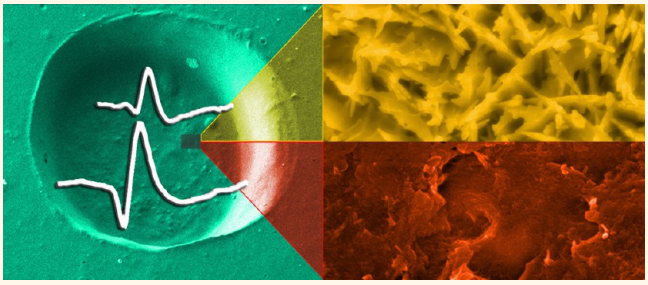

KEYWORDS: micro-electrocorticography (ECoG) · carbon nanotubes · conductive polymers · fibrin · hydrogel

Electrocorticography (ECoG) electrode arrays are frequently used in clinical practice for cortical functional mapping[1−3] or during epileptological investigations.[2,4,5] Different studies, however, pointed out how the electrodes commonly used for clinical ECoG—with their millimeter-scale size and centimeter-scale interelectrode spacing—do not provide an adequate spatial resolution for more demanding applications such as neural prosthetics.[6,7] More recent publications support the idea that closely spaced microcontacts are able to provide enough information to decode motor cortical signals,[8,9] motivating an effort to transfer such results in clinical practice.[10] The main challenge in densely packed ECoG arrays is scaling down the size and spacing of present-day clinical ECoG arrays to micrometer range while maintaining a high signal-to-noise ratio, essential for high-quality neural signal recording.

Although recent studies[11,12] reported the use of micro-electromechanical system (MEMS) processing techniques to produce ultrahigh-density arrays on flexible substrates, these electrodes, like almost all the micro-ECoG electrodes, due to their reduced contact surface, have an impedance significantly higher than standard ECoG electrodes: this hinders their ability to extract the information potentially available in neural signals.[13]

One of the most efficient ways to increase electrode charge transfer capability, while reducing their electrochemical impedance to a level sufficient to guarantee an increase in information extraction from the neural signal, is coating them with high surface area (HSA) nanomaterials.[13−19] The promising results achieved using conductive polymers,[20,21] fuzzy gold,[17,22] carbon nanotube (CNT) composites,[14,18,23] and pure CNTs[24,25] underline how the great advantage in using HSA nanocoatings is their ability to improve the recorded neural signal quality, making it possible to effectively reduce electrode size to achieve higher selectivity and sensitivity. Unfortunately, the use of nanomaterials in clinical applications raises concerns,[26−28] and finding ways to increase their safety is of paramount importance to make more widely

* Address correspondence to elisa.castagnola@iit.it; davide.ricci@iit.it.

Received for review November 6, 2012 and accepted April 16, 2013.

Published online April 16, 2013
10.1021/nn305164c

© 2013 American Chemical Society

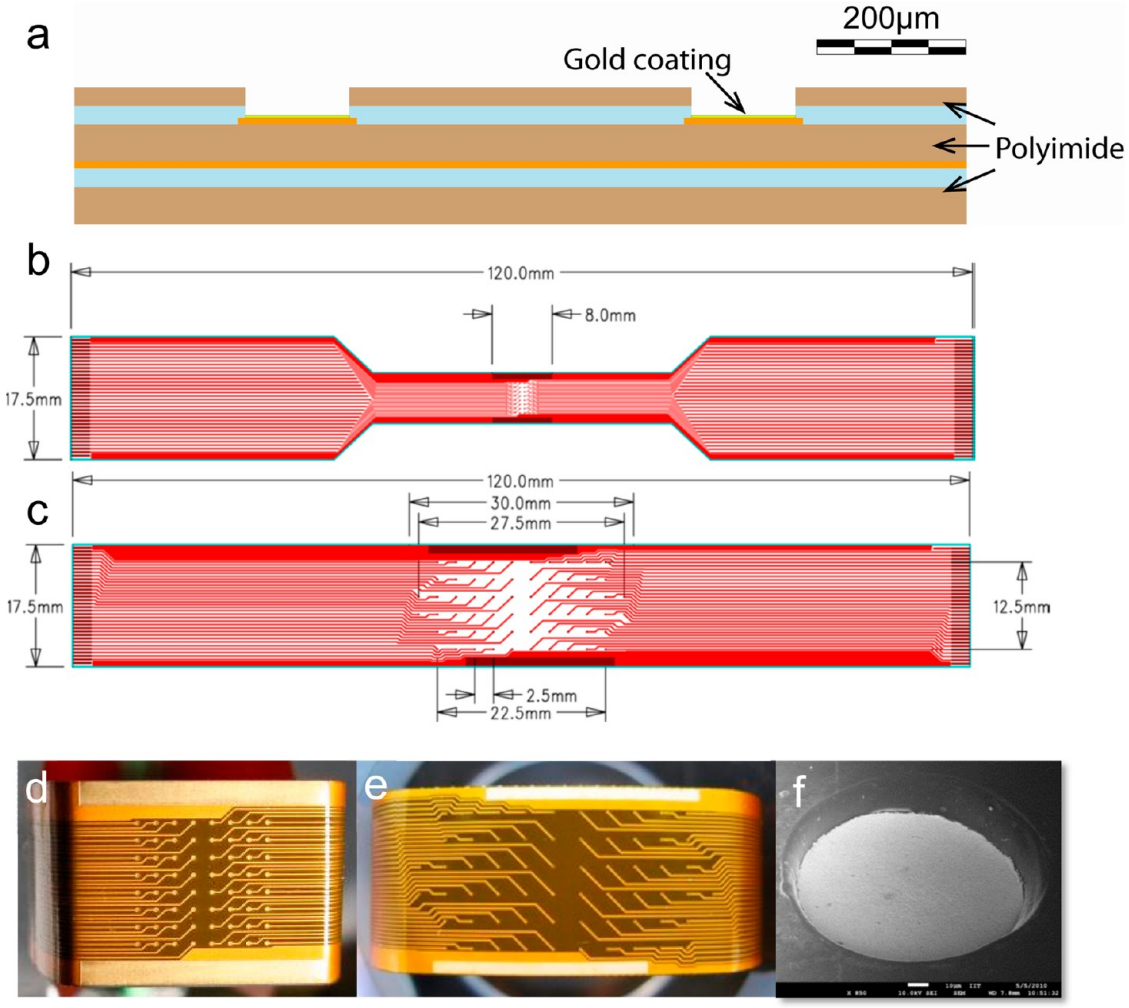

Figure 1. (a) Cross-section of a typical 64-electrode array: the base material is a 50 μm thick polyimide film coated by 9 μm copper on both faces; the superior overlay is a polyimide film (thickness, 25 μm) cold laminated over a 25 μm thick acrylic adhesive. The inferior overlay is a similar 50 μm thick film. The thickness of the gold coating is 1 μm. (b, c) Layout and dimensions of two typical electrode arrays for small (b) and large (c) total recording area. (d, e) Photographs of the arrays depicted in b and c, respectively. (f) Scanning electron microscopy images of a gold-CNT-coated recording site.

available their useful properties. In this work we introduce a method to encapsulate nanocoated neural devices with human fibrin hydrogel to create a mechanically stable barrier that avoids direct exposure of the brain to nanomaterials.

Our results open the possibility of using nanocoated densely packed low-impedance ECoG microelectrode arrays on human subjects, thus enabling the study of the information content and spatial arrangement of neural processes in the human brain with a resolution not accessible, at present, by the classical techniques of clinical neurophysiology.

RESULTS AND DISCUSSION

In order to improve the signal quality of micro-ECoG recordings in clinical neurophysiology through the use of HSA coatings, it is necessary to ensure a safe use of nanomaterials in direct contact with human tissues. Unfortunately it is difficult to estimate the maximum amount of detached material that can be accepted, and it is nearly impossible to prove that no nanoparticles detach from the nanocoated surface. For these reasons, we propose an alternative approach, *i.e.*, the encapsulation of the HSA coated devices with a proper biomaterial that maintains HSA electrophysical properties while avoiding direct exposure of the brain tissue to nanomaterials. Because our research is oriented to clinical application, among all possible hydrogels we selected human fibrin, as it is a unique surgical hemostatic/adhesive material that is extensively used in a variety of surgical situations due to its excellent biochemical and mechanical properties. Neurosurgeons are familiar with the use of fibrin sealant in clinical practice, for example, in the repair of cerebrospinal fluid leaks, sealing of vascular anastomosis sites, and hemostasis after resection of brain tumor.[29−33] As our ultimate goal is the use of micro-ECoG arrays during human brain surgery, this approach is particularly attractive,

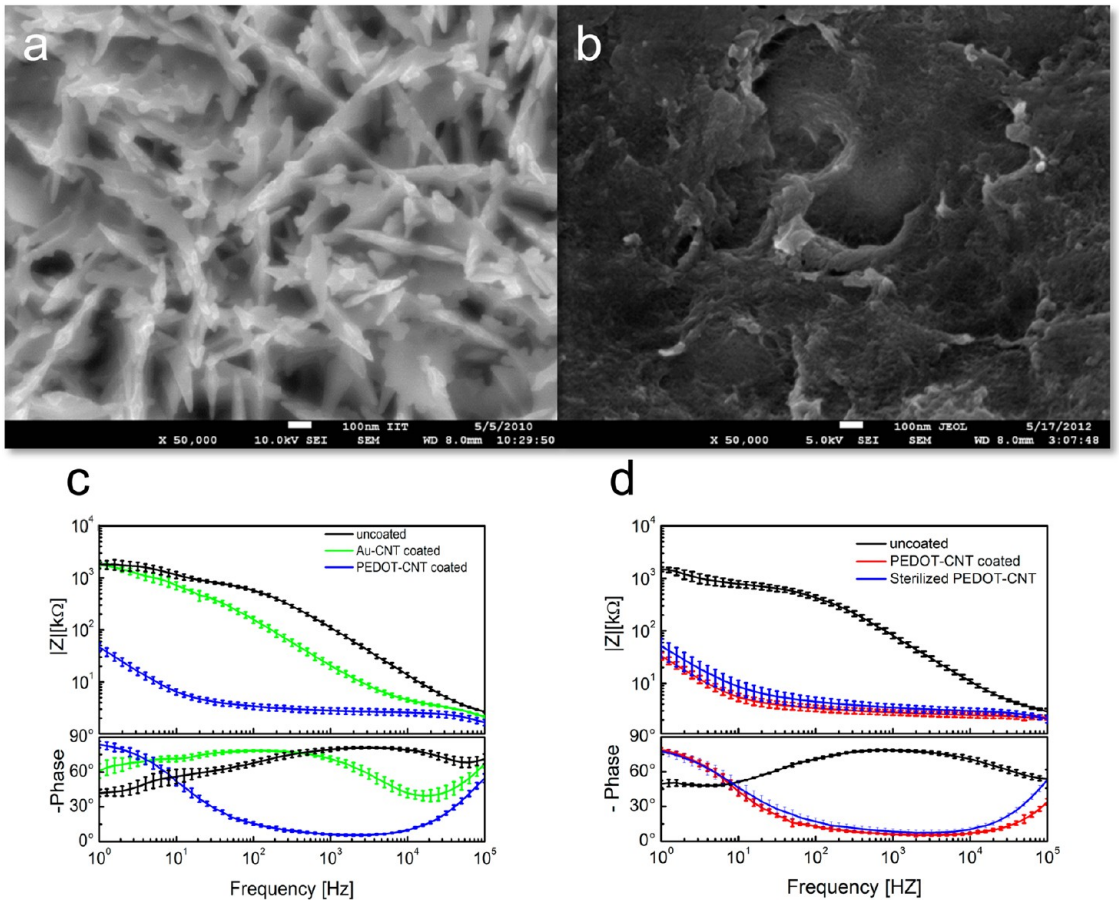

Figure 2. Scanning electron micrographs of the surface of (a) gold-CNT- and (b) PEDOT-CNT-coated electrodes. (c) Impedance spectra of uncoated (black), gold-CNT-coated (green), and PEDOT-CNT-coated (blue) electrodes (mean and standard deviation of 64 recording sites for each coating). (d) Impedance spectra of a micro-ECoG electrode array coated with PEDOT-CNTs before (red) and after (blue) steam sterilization (mean and standard deviation of 64 recording sites for each coating). The impedance spectra of the uncoated microelectrodes are reported as reference (black).

also considering that autologous fibrin hydrogel can be obtained from the patient's own blood, thus reducing to a minimum infection risks.

To demonstrate the effectiveness of this approach, we designed a family of ECoG devices based on the commercially available flexible printed circuit (FPC) technology, with 64 recording sites (140 μm in diameter, Figure 1), post-processed in our laboratory by electrodepositing a nanocomposite of poly(3,4-ethylenedioxythiophene) (PEDOT) and carbon nanotubes in order to reduce electrode impedance and achieve a better signal-to-noise ratio.[19] The electrodes—obtained by laser ablation of the polyimide layer insulating a standard copper FPC substrate (9 μm thick), passivated by gold electroplating (1 μm thick)—were electrocoated with a gold-CNT layer that acts as an adhesion layer[22] for the PEDOT-CNT composite. Some examples of scanning electron micrographs (SEM) of the gold-CNT- and PEDOT-CNT-coated electrode morphologies are shown in Figure 2. The gold-CNT coating (Figure 2a) presents a nanorough surface, formed by nanosized gold lamellas, that reduces the electrode impedance by two-thirds with respect to the uncoated one (100 Hz, LFP center band). The PEDOT-CNT composite coating (Figure 2b) presents a compact sponge-like morphology that allows obtaining an impedance reduction up to more than 2 orders of magnitude over the frequency range of interest (1 Hz to 10 kHz) and especially at the frequency of 100 Hz (Figure 2c). The impedance values, obtained by averaging all 64 electrodes of a micro-ECoG array, are 571.01 $\pm$ 39.39 kΩ (mean $\pm$ standard deviation) for the uncoated ones, 157.14 $\pm$ 22.63 kΩ for gold-CNTs, and 3.41 $\pm$ 0.45 kΩ for PEDOT-CNTs.

To be compliant with clinical use, such devices have to withstand the usual sterilization processes. We decided to focus our attention on the most common sterilization process used in hospitals, *i.e.*, steam under pressure. We found that our PEDOT-CNT-coated devices are fully compatible with a sterilization process in saturated water vapor at 122 °C and 2 atm for 20 min. The magnitude of the impedance spectra of micro-ECoG arrays coated with PEDOT-CNTs (2.7 $\pm$ 0.3 kΩ @ 100 Hz, mean $\pm$ standard deviation over 64 electrodes) does not change significantly after the sterilization (4.4 $\pm$ 0.9 kΩ @ 100 Hz), remaining 2 orders of magnitude lower than that of the

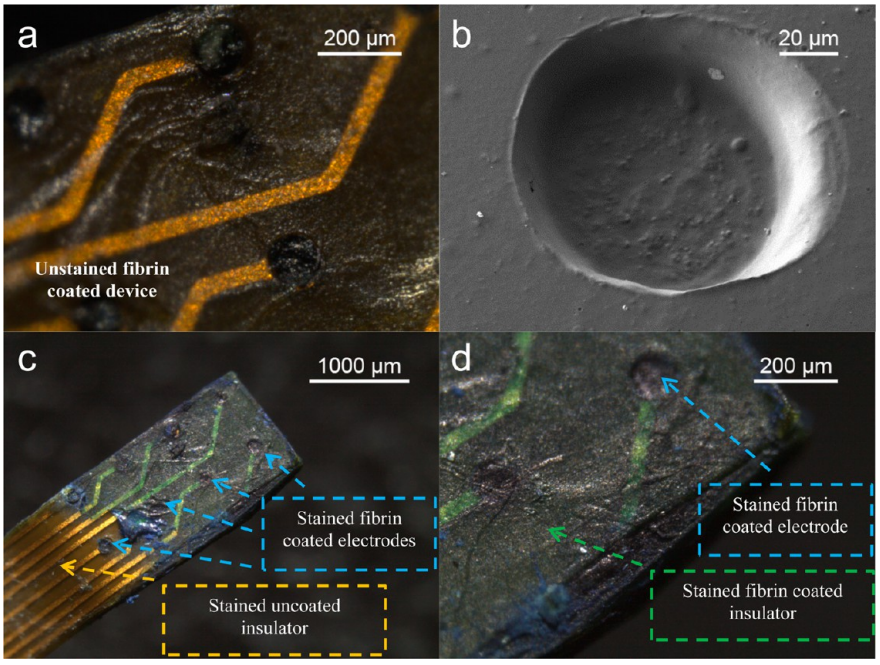

Figure 3. (a) Optical image of a flexible micro-ECoG array coated with PEDOT-CNT nanocomposite and encapsulated with fibrin. (b) SEM image of a single recording/stimulation site encapsulated with fibrin (the sample is dehydrated). (c, d) Optical images of a flexible micro-ECoG subarray coated with PEDOT-CNT, encapsulated with fibrin and stained with methylene blue, after a recording session from rat somatosensory cortex.

uncoated electrodes (428.6 ± 51.3 kΩ @ 100 Hz). Full impedance spectra are reported in Figure 2d.

As discussed before, given the impossibility to reach absolute confidence that no nanoparticle detaches during contact with the brain surface, we propose encapsulating the HSA-coated electrodes with a highly biocompatible hydrogel: human fibrin. We used a commercially available two-component fibrin sealant that is approved both in Europe and in the United States as a surgical specialty (TISSEEL [fibrin sealant], Baxter, USA) and is commonly used in neurosurgical practice. Our choice was to develop a procedure compliant with the protocols, approved by the competent medical surveillance agencies, for the safe handling and use of fibrin in sterile operating theaters. This is the main reason that we devised a process that requires only the sterilization of the micro-ECoG array before introducing it in a sterile environment, while the fibrin is placed on the device by the surgeon just before use, so that the safety of the protein is not compromised by an external manipulation. Moreover, fibrin hydrogel, during the sterilization process, would denature and dry, causing cracks on its surface that would seriously affect the coating integrity and thus the device safety.

We proceeded as follows: after the PEDOT-CNT coating deposition and the electrochemical validation of the device, we subjected it to the sterilization protocol. The fibrinogen and the thrombin are prepared according to a standard procedure and then deposited on the surface of the device, forming the protection layer. To apply fibrin, we place the array on a hot plate at 37 °C (to promote the reaction) and deposit a thin layer of fibrinogen (sealer protein) on our device using a spatula. The depth of the openings in the polyimide layer (25 μm) ensure the minimum thickness of the coating. The thrombin is then dropped over this layer and allowed to diffuse for about 5 min, forming a thin fibrin layer adhering to the array. The excess thrombin is removed by rinsing in ultrapure water.

Optical images of a micro-ECoG array coated with PEDOT-CNT nanocomposite after fibrin encapsulation and a SEM image of a dried fibrin-encapsulated electrode are reported in Figure 3. Fibrin encapsulation does not change significantly the impedance spectra of both uncoated (from 591.4 ± 58.2 kΩ to 525.21 ± 61.7 kΩ @ 100 Hz, Figure 4a) and PEDOT-CNT-coated microelectrodes (from 3.4 ± 0.2 kΩ to 3.9 ± 0.4 kΩ @ 100 Hz, Figure 3b), demonstrating that the fibrin hydrogel is a good ionic conductor. The small decrease of impedance that occurs in the case of uncoated electrodes can be justified by the extreme difference in wettability of the surface materials; in fact, the water contact angle on the pristine surface of the polyimide insulation was 80.47 ± 7.48°, while on the fibrin-coated surface it was 3.75 ± 0.83°.

To establish whether these fibrin-encapsulated electrodes can be suitable for cortical stimulation too, we investigated their ability to withstand current stimulation patterns. The ability of PEDOT-CNT coating to resist intense and prolonged current stimulation patterns was verified by repeatedly applying a series of one million pulses (Table 1, pattern 1) and measuring

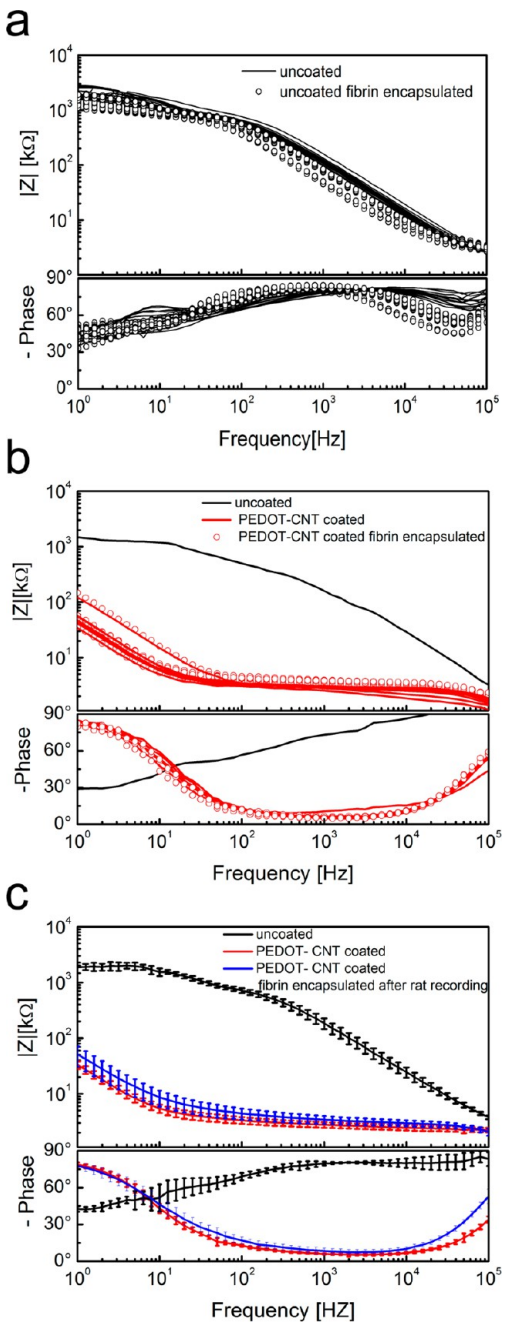

Figure 4. (a) Impedance spectra of the recording sites of an uncoated micro-ECoG array (140 μm diameter electrodes) before (continuous line) and after (circles) fibrin deposition. (b) Impedance spectra of the recording sites of a similar micro-ECoG array coated with PEDOT-CNTs before (continuous red line) and after (red circles) fibrin deposition; the black line shows the typical impedance spectra of an uncoated microelectrode. (c) Impedance spectra of a micro-ECoG eight-electrode subarray coated with PEDOT-CNTs before (in red) and after fibrin deposition and recording from rat brain (in blue).

whether there was any change in impedance spectra after each series. The impedance spectra do not change even after four such series (see Figure S1 in the Supporting Information). We then checked if the fibrin layer of encapsulated electrodes is affected by the current passage. We tested both uncoated and PEDOT-CNT-coated micro-ECoG arrays, as we expect changes in behavior due to the different impedance and the consequent different voltage drop at the electrode−hydrogel interface. We applied the same stimulation pattern as before and then a stimulation pattern having current pulses 10 times greater (Table 1, pattern 2). After each pulse series the impedance was measured and the integrity of the fibrin layer was checked optically. In the case of the fibrin-encapsulated uncoated electrode we found a change in impedance (from 491.4 ± 463 kΩ to 249.1 ± 46.3 kΩ @ 100 Hz) after the first series (pattern 1), and then the impedance stabilized (Figure S2a in Supporting Information). Unfortunately the optical check clearly shows cracks and formation of gas bubbles in the fibrin layer that can be easily explained by faradaic reactions occurring at the interface. Applying the same stimulation patterns at the fibrin-encapsulated PEDOT-CNT-coated array, we did not observe any significant change in impedance (varying from 6.5 ± 1.6 kΩ @ to 6.9 ± 2.7 @ kΩ 100 Hz; see Figure S2b in the Supporting Information for the spectra), and no modification of the fibrin layer was observed.

TABLE 1. Stimulation Patterns

	number of pulses	chatodic pulse duration	period	charge density
pattern 1	1 million	500 μS	2 ms	5.7 mC·cm^{-2}
pattern 2	1 million	500 μS	2 ms	57 mC·cm^{-2}

We tested our devices *in vivo* by recording signals from rat somatosensory cortex using *ad hoc* tailored microelectrode subarrays (4 by 2 electrodes), connected to custom electronics.[34,35] Somatosensory-evoked potentials (SEPs) were elicited through multiwhisker deflection obtained by a vibrating system that stimulated the whiskers along the horizontal plane.

The impedance spectra of the electrodes before (3.9 ± 0.3 kΩ @ 100 Hz) and after (6.2 ± 1.0 kΩ @ 100 Hz) two 15 min long epi-cortical recording sessions on rat brain do not change significantly (Figure 4c), giving first evidence of the stability of the fibrin. The state of the fibrin layer after this test was verified optically by staining micro-ECoG arrays with 1% methylene blue solution (MarcoViti Farmaceutica S.p.A., Italy), as it is selectively absorbed by fibrin[36,37] and not by the other materials used in our device. We found that, after the recordings, the fibrin coating was still in place firmly adhering to the recording sites (Figure 3c, d), thus effectively protecting the tissues from direct contact with the nanostructured coating.

Examples of SEPs recorded in response to a multiwhisker deflection using an uncoated electrode array, a PEDOT-CNT-coated one, and the same array after fibrin encapsulation are reported in Figure 5. The graphs shown are based on the average of the signals recorded during the 10 iterations of the whisker stimulation scheme of one 15 min session and from four electrodes for each array. The response to the whole

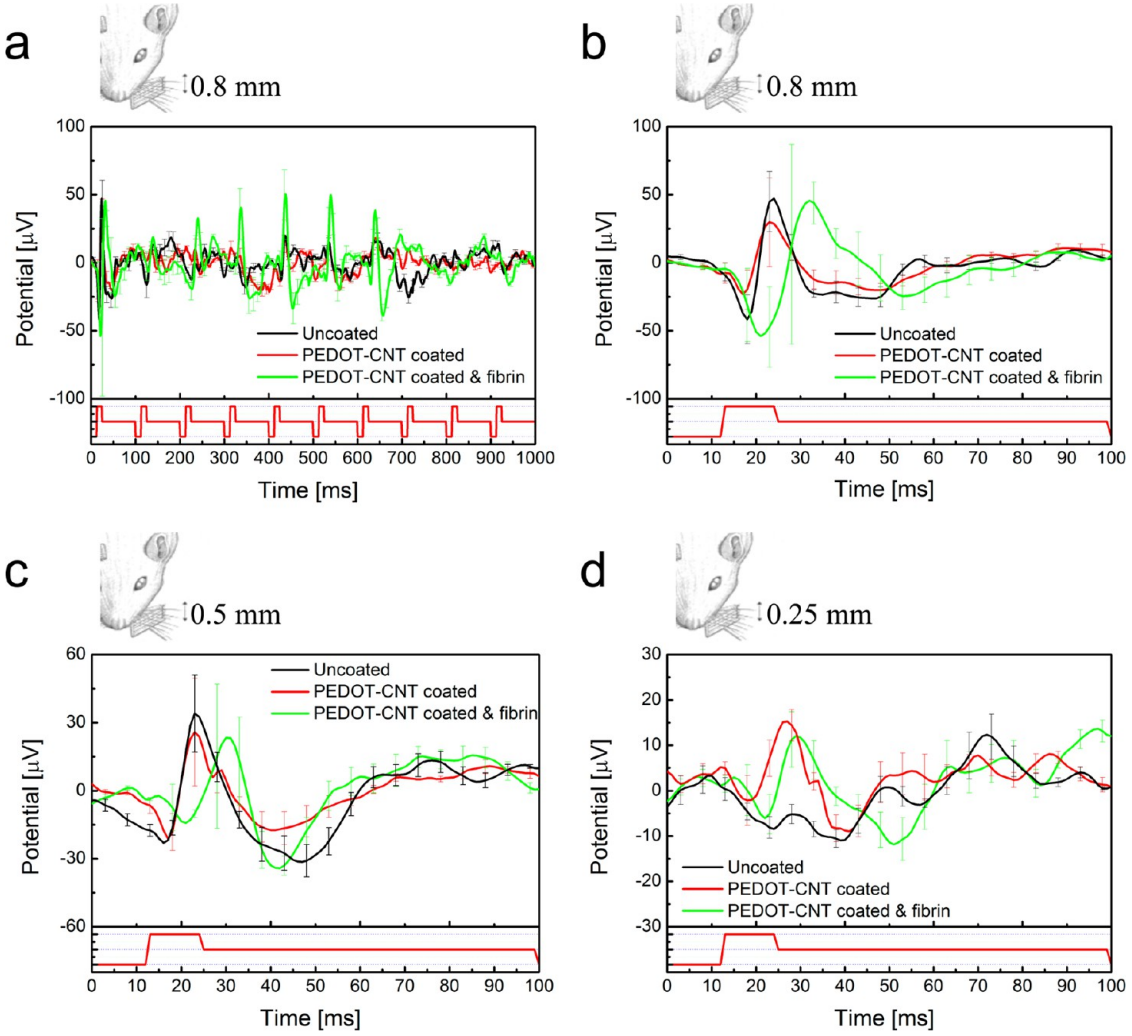

Figure 5. (a) Averaged somatosensory-evoked potentials ($n = 10$) recorded in response to a multiwhisker deflection of 0.8 mm from rat somatosensory cortex during whisker mechanical stimulation (10 Hz) using the uncoated (black), PEDOT-CNT-coated (red), and fibrin-encapsulated PEDOT-CNT-coated (green) microelectrode arrays. Response to the first 12 ms truncated Gaussian of the 10 Hz train to a multiwhisker deflection of (b) 0.8 mm, (c) 0.5 mm, and (d) 0.25 mm (rat whisker stimulation drawing adapted from Lak *et al.*, 2010).

TABLE 2. Amplitude of the SEP Response at the First Stimulus

deflection	uncoated	PEDOT-CNT	PEDOT-CNT + fibrin
0.8 mm	88.7 μV	52.9 μV	99.6 μV
0.5 mm	62.6 μV	46.8 μV	37.5 μV
0.25 mm		17.3 μV	18.1 μV

stimulation train is reported in Figure 5a, while Figure 5b, c, and d highlight the response to the first truncated Gaussian[38] of the 10 Hz trains while varying the deflection amplitude (0.8, 0.5, and 0.25 mm, respectively).

The electrode performance in recording SEP signals can be properly evaluated by assessing which is the smallest whisker deflection that generates a SEP signal that can be detected using a given electrode. As it can be observed from the mean amplitude of the response to the first stimulus (Table 2), in spite of the maximum amplitude of recorded signals, PEDOT-CNT-coated electrodes, with or without fibrin, are able to record SEP signals corresponding to a whisker stimulation 50% smaller than in the case of uncoated electrodes. These results prove that the fibrin-encapsulated PEDOT-CNT-coated electrodes provide high-quality ECoG signal recordings.

CONCLUSIONS

In summary, the present work provides a reliable technique for multielectrode micro-ECoG recording and stimulation in humans by combining (i) the versatility of flexible printed circuit boards, (ii) electrochemical performances of CNT-based electrodeposited nanocoatings, and (iii) the biocompatibility of human fibrin electrode encapsulation. PEDOT-CNT nanocomposites are electrodeposited on micro-ECoG arrays, obtaining high surface area nanocoatings that significantly reduce microelectrode impedance, with an electrochemical conductivity

improvement—at 100 Hz—of 2 orders of magnitude. We demonstrated that it is possible to cover these devices with a human fibrin hydrogel to create a mechanically stable barrier that avoids direct exposure of the brain to the nanocoatings. The fibrin encapsulation does not interfere with the electrochemical performance of the electrodes and is not damaged/deteriorated by current stimulation patterns. Finally, we proved that fibrin-coated devices are capable of recording neural signals from rat somatosensory cortex with performances that are at least as good as the same devices without fibrin. Our method allows taking advantage of all the improvements in terms of signal power, signal-to-noise ratio, and spatial and temporal resolution that derive from the use of nanocoatings, avoiding direct exposure of the brain tissue to the nanomaterial itself.

In conclusion, this novel technique opens the possibility of using nanocoated densely packed ECoG microelectrode arrays on human subjects, thus enabling the study of the information content and spatial arrangement of neural processes in the human brain with a resolution not accessible, at present, with classical clinical neurophysiology techniques.

METHOD

Electrocorticography Devices. The base material was a polyimide film (50 μm thick) covered on both sides by a copper foil (9 μm thick). After the lithographic processing, FPCs were isolated by a cold laminated polyimide overlay (25 μm thick on the front side, 50 μm thick on the back side), and 64 recording sites (140 μm in diameter) were then created by laser ablation of the polyimide layer. After electrode fabrication, the exposed copper was passivated by gold electroplating (1 μm thick).

Gold-CNT Electrochemical Co-deposition. The gold and CNT nanocomposite (gold-CNT) was co-electrodeposited starting from a 10 mM potassium dicyanoaurate(I) (Sigma-Aldrich, USA) aqueous solution containing 1.5 mg·mL^{-1} of multiwalled CNTs (NC 3100, thin MWCNT 95+% carbon purity, Nanocyl S.A. Belgium) partially dispersed by a sonotrode (4 W·mL^{-1} peak power pulses, 6 s at 66% duty cycle for 1 min), by applying monophasic voltage pulses (0.2−1.0 V, 240 s, duty cycle 50%) on the electrode array, while keeping the solution at 45 °C. Depositions were carried out using a potentiostat/galvanostat (PARSTAT 2273, Princeton Applied Research, Oak Ridge, TN, USA) connected to a three-electrode electrochemical cell with a platinum counter electrode and a Ag/AgCl reference electrode.

PEDOT-CNT Electrochemical Co-depositions. Poly(3,4-ethylenedioxythiophene) (PEDOT) and carboxylated MWCNTs (COOH-CNTs, NC 3151, <4% of −COOH functional groups, Nanocyl S.A., Belgium) nanocomposites (PEDOT-CNT) were co-electrodeposited from a 0.5 M 3,4-ethylenedioxythiophene (EDOT, Sigma-Aldrich, USA) aqueous solution containing 1 mg·mL^{-1} of suspended COOH-CNTs and 0.6 wt % of poly(sodium 4-styrenesulfonate) (PSS, Sigma-Aldrich USA). COOH-CNTs were suspended in ultrapure water (Milli-Q, Millipore) by horn sonication (6 s at 66% duty cycle pulses, 4 W·mL^{-1}) for 30 min while keeping the solution cooled with an ice bath. PSS and the monomer were added to the suspension immediately afterward, and the solution was kept deoxygenated by bubbling nitrogen. The electrochemical deposition was carried out in inert atmosphere in potentiostatic mode at constant temperature (ice bath, 0 °C). The polymerization potential was set to 0.8 V *versus* reference electrode. PEDOT-CNT nanocomposite coatings were electrodeposited using 5 C·cm^{-2}. Depositions were carried out using a potentiostat/galvanostat (PARSTAT 2273, Princeton Applied Research) connected to a three-electrode electrochemical cell with a platinum counter electrode and a Ag/AgCl reference electrode.

Electrochemical Impedance Spectroscopy. The impedance of the microelectrodes was measured by galvanostatic electrochemical impedance spectroscopy (GEIS), performed in saline (0.9% NaCl), by applying a current (sine wave) of 300 nA RMS at 10 frequencies per decade over the range 1−10^5 Hz. GEIS was carried out using a potentiostat/galvanostat (PARSTAT 2273, Princeton Applied Research) connected to a three-electrode electrochemical cell with a platinum counter electrode and a Ag/AgCl reference electrode.

Stimulation Test. The microelectrode stimulation tests were performed in saline (0.9% NaCl) by applying two different stimulation patterns (see Table 1) of cathodic first charge balanced biphasic current pulses. Stimulation tests were carried out using a potentiostat/galvanostat (PARSTAT 2273, Princeton Applied Research) connected to a three-electrode electrochemical cell with a platinum counter electrode and a Ag/AgCl reference electrode.

Fibrin Layer Deposition. To deposit the fibrin layer, the polyimide-based FPC circuits were placed over an aluminum block heated at 37 °C. Meanwhile, the fibrin precursors, fibrinogen and thrombin (see http://www.baxter.com/downloads/healthcare_professionals/products/Tisseel_PI.pdf for the description), were warmed to the same temperature. The fibrinogen was spread over the electrodes with a spatula, and, then, a large thrombin drop was placed over the whole fibrinogen-coated surface. After 5 min, a stable fibrin layer was formed and the micro-ECoG array was rinsed in ultrapure water to remove the residual thrombin solution.

Fibrin Staining. In order to optically verify the state of the fibrin after stimulation and recording tests through a microscope (Leica Z16 Apo, Leica Microsystems), we stained the micro-ECoG arrays with 1% methylene blue solution (MarcoViti Farmaceutica S.p.A., Italy), as it is selectively absorbed by fibrin[36,37] and not by the other materials used in our device. We dipped the electrode in the 1% methylene blue solution and then rinsed with ultrapure deionized water (Milli-Q, Millipore).

Neural Recordings in Rat Brain. The experiments were carried out on Long-Evans rats under anesthesia. Each animal was positioned on a stereotactic frame (Kopf, Tujunga, CA, USA), and a small craniotomy was made in the parietal bone in order to expose the *vibrissa* region of somatosensory cortex where *dura mater* was left intact. The microelectrode array was placed over the cortex, between the bone and the *dura mater*, to record somatosensory-evoked potentials elicited through multiwhisker deflection. Each ECoG array was tested in two different cortex positions by two consecutive recording sessions of 15 min each. All surgical procedures were performed in compliance with the Italian law regarding the care and use of experimental animals (DL116/92) and approved by the Italian Institute of Technology Animal Use Committee and by the Italian Ministry of Health.

Whisker Deflections. The multiwhisker deflection was performed by controlling a vibrating system that permits stimulating the whisker pad along the horizontal plane using different stimulation patterns. The whiskers, contralateral to the recorded cortex, were cut 1 cm from the base and included in a Velcro strip attached to a rod moved by a shaker (Type 4810 minishaker; Bruel & Kjaer) controlled by a National Instruments board (Austin, TX, USA). The deflection stimulus consisted of 10 trains of 10 truncated Gaussians[38] of 12 ms duration at 10 Hz followed by a 5 s pause. The amplitude of the stimulus was changed after each train in order to obtain multiwhisker deflections respectively of 150, 200, 250, 500, and 800 μm.

Neural Recording System. To record spontaneous and stimulus-induced neural activity, we developed a compact 16-channel recording system that includes a headstage, a control unit, and acquisition software. The electronics for the headstage primarily consists of two identical integrated circuits (IC), both packaged

in a 32-pin low-profile quad flat package, previously described in the companion papers.[34,35] Briefly, each IC includes eight low-noise amplifiers that have 2 μVrms input referred noise, 56 dB gain, 3 Hz to 10 kHz bandwidth, and 12 μW @ 3.3 V power consumption. The eight raw traces coming from the headstage are fed into the control unit for further user-programmable signal conditioning. In particular, each channel is low pass filtered with a fourth-order filter whose cutoff frequency is set to 8 kHz, while a first-order 3 Hz high-pass filter removes any dc component from the recorded traces before further user-programmable gain amplification. Notice that data presented in this work were acquired with a total gain of 62 dB. The amplified signals are multiplexed and digitally converted (10 bit, 40 ksample/s). A commercial FPGA from Opal Kelly, based on a Xilinx Spartan-3E integrated chip, was used for digital processing of the multiplexed signal as well as for USB interface with a personal computer. Finally, LabView (National Instruments, Austin, TX, USA)-based acquisition software was used for real-time data storage and visualization. As the system is battery powered, electrical isolation was guaranteed, while a Faraday cage allowed removing main noise components.

Conflict of Interest: The authors declare no competing financial interest.

Acknowledgment. This work was supported by the BMI project of the Robotics, Brain and Cognitive Sciences Department, Istituto Italiano di Tecnologia.

Supporting Information Available: An expanded description of experimental procedures and characterizations is given. This material is available free of charge *via* the Internet at http://pubs.acs.org.

REFERENCES AND NOTES

1. Ritaccio, A.; Brunner, P.; Cervenka, M. C.; Crone, N.; Guger, C.; Leuthardt, E.; Oostenveld, R.; Stacey, W.; Schalk, G. Proceedings of the First International Workshop on Advances in Electrocorticography. *Epilepsy Behav.* **2010**, *19*, 204–215.
2. Ritaccio, A.; Boatman-Reich, D.; Brunner, P.; Cervenka, M. C.; Cole, A. J.; Crone, N.; Duckrow, R.; Korzeniewska, A.; Litt, B.; Miller, K. J.; *et al*. Proceedings of the Second International Workshop on Advances in Electrocorticography. *Epilepsy Behav.* **2011**, *22*, 641–650.
3. Gharabaghi, A.; Samii, A.; Koerbel, A.; Rosahl, S. K.; Tatagiba, M.; Samii, M.; Bricolo, A.; Porter, R. W.; Spetzler, R. F.; Briggs, R.; *et al*. Preservation of Function in Vestibular Schwannoma Surgery. *Neurosurgery* **2007**, *60*, 124–128.
4. Wyler, A. R.; Ojemann, G. A.; Lettich, E.; Ward, A. A. Subdural Strip Electrodes for Localizing Epileptogenic Foci. *J. Neurosurg.* **1984**, *60*, 1195–1200.
5. Dümpelmann, M.; Fell, J.; Wellmer, J.; Urbach, H.; Elger, C. E. 3D Source Localization Derived from Subdural Strip and Grid Electrodes: a Simulation Study. *Clin. Neurophysiol.* **2009**, *120*, 1061–1069.
6. Menon, V.; Freeman, W. J.; Cutillo, B. A.; Desmond, J. E.; Ward, M. F.; Bressler, S. L.; Laxer, K. D.; Barbaro, N.; Gevins, A. S. Spatio-Temporal Correlations in Human Gamma Band Electrocorticograms. *Electroencephalogr. Clin. Neurophysiol.* **1996**, *98*, 89–102.
7. Towle, V. L.; Syed, I.; Berger, C.; Grzesczcuk, R.; Milton, J.; Erickson, R. K.; Cogen, P.; Berkson, E.; Spire, J. P. Identification of the Sensory/Motor Area and Pathologic Regions Using ECoG Coherence. *Electroencephalogr. Clin. Neurophysiol.* **1998**, *106*, 30–39.
8. Leuthardt, E. C.; Freudenberg, Z.; Bundy, D.; Roland, J. Microscale Recording from Human Motor Cortex: Implications for Minimally Invasive Electrocorticographic Brain-Computer Interfaces. *Neurosurg. Focus* **2009**, *27*, E10.
9. Kellis, S. S.; House, P. A.; Thomson, K. E.; Brown, R.; Greger, B. Human Neocortical Electrical Activity Recorded on Nonpenetrating Microwire Arrays: Applicability for Neuroprostheses. *Neurosurg. Focus* **2009**, *27*, E9.
10. Stead, M.; Bower, M.; Brinkmann, B. H.; Lee, K.; Marsh, W. R.; Meyer, F. B.; Litt, B.; Van Gompel, J.; Worrell, G. A. Microseizures and the Spatiotemporal Scales of Human Partial Epilepsy. *Brain* **2010**, *133*, 2789–2797.
11. Hollenberg, B. A; Richards, C. D.; Richards, R.; Bahr, D. F.; Rector, D. M. A MEMS Fabricated Flexible Electrode Array for Recording Surface Field Potentials. *J. Neurosci. Methods* **2006**, *153*, 147–153.
12. Rubehn, B.; Bosman, C.; Oostenveld, R.; Fries, P.; Stieglitz, T. A MEMS-Based Flexible Multichannel ECoG-Electrode Array. *J. Neural Eng.* **2009**, *6*, 36003.
13. Cheung, K. C. Implantable Microscale Neural Interfaces. *Biomed. Microdevices* **2007**, *9*, 923–938.
14. Jan, E.; Hendricks, J. L.; Husaini, V.; Richardson-Burns, S. M.; Sereno, A.; Martin, D. C.; Kotov, N. A. Layered Carbon Nanotube-Polyelectrolyte Electrodes Outperform Traditional Neural Interface Materials. *Nano Lett.* **2009**, *9*, 4012–4018.
15. Cogan, S. F. Neural Stimulation and Recording Electrodes. *Annu. Rev. Biomed. Eng.* **2008**, *10*, 275–309.
16. Castagnola, E.; Ansaldo, A.; Fadiga, L.; Ricci, D. Chemical Vapour Deposited Carbon Nanotube Coated Microelectrodes for Intracortical Neural Recording. *Phys. Status Solidi (B)* **2010**, *247*, 2703–2707.
17. Ferguson, J. E.; Boldt, C.; Redish, A. D. Creating Low-Impedance Tetrodes by Electroplating with Additives. *Sens. Actuators, A* **2009**, *156*, 388–393.
18. Keefer, E. W.; Botterman, B. R.; Romero, M. I.; Rossi, A. F.; Gross, G. W. Carbon Nanotube Coating Improves Neuronal Recordings. *Nat. Nanotechnol.* **2008**, *3*, 434–439.
19. Kotov, N. A.; Winter, J. O.; Clements, I. P.; Jan, E.; Timko, B. P.; Campidelli, S.; Pathak, S.; Mazzatenta, A.; Lieber, C. M.; Prato, M.; *et al*. Nanomaterials for Neural Interfaces. *Adv. Mater.* **2009**, *21*, 3970–4004.
20. Cui, X.; Hetke, J. F.; Wiler, J. A.; Anderson, D. J.; Martin, D. C. Electrochemical Deposition and Characterization of Conducting Polymer Polypyrrole/PSS on Multichannel Neural Probes. *Sens. Actuators, A* **2001**, *93*, 8–18.
21. Ludwig, K. A.; Uram, J. D.; Yang, J.; Martin, D. C.; Kipke, D. R. Chronic Neural Recordings Using Silicon Microelectrode Arrays Electrochemically Deposited with a Poly(3,4-ethylenedioxythiophene) (PEDOT) Film. *J. Neural Eng.* **2006**, *3*, 59–70.
22. Cui, X.; Martin, D. C. Fuzzy Gold Electrodes for Lowering Impedance and Improving Adhesion with Electrodeposited Conducting Polymer Films. *Sens. Actuators, A* **2003**, *103*, 384–394.
23. Green, R. A; Williams, C. M.; Lovell, N. H.; Poole-Warren, L. A. Novel Neural Interface for Implant Electrodes: Improving Electroactivity of Polypyrrole through MWNT Incorporation. *J. Mater. Sci.* **2008**, *19*, 1625–1629.
24. Ansaldo, A.; Castagnola, E.; Maggiolini, E.; Fadiga, L.; Ricci, D. Superior Electrochemical Performance of Carbon Nanotubes Directly Grown on Sharp Microelectrodes. *ACS Nano* **2011**, *5*, 2206–2214.
25. Shoval, A.; Adams, C.; David-Pur, M.; Shein, M.; Hanein, Y.; Sernagor, E. Carbon Nanotube Electrodes for Effective Interfacing with Retinal Tissue. *Front. Neuroeng.* **2009**, *2*, 4.
26. Oberdörster, G.; Maynard, A.; Donaldson, K.; Castranova, V.; Fitzpatrick, J.; Ausman, K.; Carter, J.; Karn, B.; Kreyling, W.; Lai, D.; *et al*. Principles for Characterizing the Potential Human Health Effects from Exposure to Nanomaterials: Elements of a Screening Strategy. *Part. Fibre Toxicol.* **2005**, *2*, 8.
27. Resnik, D. B.; Tinkle, S. S. Ethical Issues in Clinical Trials Involving Nanomedicine. *Contemp. Clin. Trials* **2007**, *28*, 433–441.
28. Sahoo, S. K.; Parveen, S.; Panda, J. J. The Present and Future of Nanotechnology in Human Health Care. *Nanomedicine* **2007**, *3*, 20–31.
29. Spotnitz, W. D. Fibrin Sealant: Past, Present, and Future: a Brief Review. *World J. Surg.* **2010**, *34*, 632–634.
30. Radosevich, M.; Goubran, H. A.; Burnouf, T. Fibrin Sealant: Scientific Rationale, Production Methods, Properties, and Current Clinical Use. *Vox Sang.* **1997**, *72*, 133–143.
31. Lee, K. C.; Park, S. K.; Lee, K. S. Neurosurgical Application of Fibrin Adhesive. *Yonsei Med. J.* **1991**, *32*, 53–57.

32. Janmey, P. A.; Winer, J. P.; Weisel, J. W. Fibrin Gels and Their Clinical and Bioengineering Applications. *J. R. Soc., Interface* **2009**, *6*, 1–10.
33. Buchta, C.; Hedrich, H. C.; Macher, M.; Höcker, P.; Redl, H. Biochemical Characterization of Autologous Fibrin Sealants Produced by CryoSeal and Vivostat in Comparison to the Homologous Fibrin Sealant Product Tissucol/Tisseel. *Biomaterials* **2005**, *26*, 6233–6241.
34. Bonfanti, A.; Borghi, T.; Gusmeroli, R.; Zambra, G.; Oliyink, A.; Fadiga, L.; Spinelli, A. S.; Baranauskas, G. A Low-Power Integrated Circuit for Analog Spike Detection and Sorting in Neural Prosthesis Systems. *IEEE Proc. BioCAS* **2008**, 257–260.
35. Borghi, T.; Bonfanti, A.; Gusmeroli, R.; Zambra, G.; Spinelli, A. S. A Power-Efficient Analog Integrated Circuit for Amplification and Detection of Neural Signals. *IEEE Proc. EMBS* **2008**, 4911–4915.
36. Gitlin, D.; Craig, J. M. Variations in the Staining Characteristics of Human Fibrin. *Am. J. Pathol.* **1957**, *33*, 267–283.
37. Singer, M. The Staining of Basophilic Components. . *Histochem. Cytochem.* **1954**, *2*, 322–333.
38. Lak, A.; Arabzadeh, E.; Harris, J. A.; Diamond, M. E. Correlated Physiological and Perceptual Effects of Noise in a Tactile Stimulus. *Proc. Natl. Acad. Sci. U.S.A.* **2010**, *107*, 7981–7986.